

- Polyclonal rabbit antibodies were obtained after three or four immunizations with both *E. coli*- and baculovirus-expressed DmORC2. These polyclonal antibodies were affinity-purified (21) by incubation with baculovirus-produced DmORC2 protein coupled to Reactigel beads (Pierce). The eluted antibodies were bound to protein A-Sepharose (Pharmacia) and chemically cross-linked to this support with dimethylpimelidate (27). For immunoprecipitation, 1  $\mu$ l of these beads was added directly to the respective chromatographic or glycerol gradient fraction, adjusted to 100 mM KCl, incubated for 2 hours at 4°C, and washed six times with 0.1 M KCl-HEMG [25 mM Hepes (pH 7.6), 0.5 mM EDTA, 12.5 mM MgCl<sub>2</sub>, and 10% glycerol] (14). The recovered material was resuspended directly in SDS sample buffer and analyzed by SDS-PAGE.
13. U. Heberlein and R. Tjian, *Nature* **331**, 410 (1988).
  14. *Drosophila* Genome Center, Lawrence Berkeley Laboratory, Berkeley, CA; GenBank accession number L39626.
  15. E. V. Koonin, *Nucleic Acids Res.* **21**, 2541 (1993).
  16. S. K. Hansen, D. T. S. Pak, M. Gossen, S. Zhou, M. R. Botchan, unpublished data.
  17. A. E. Ehrenhofer-Murray, M. Gossen, D. T. S. Pak, M. R. Botchan, J. Rine, *Science* **270**, 1671 (1995).
  18. V. E. Foe, G. M. Odell, B. A. Edgar, in *The Development of Drosophila melanogaster*, M. Bate and A. M. Arias, Eds. (Cold Spring Harbor Laboratory Press, Cold Spring Harbor, NY, 1993), vol. 1, pp. 149–300.
  19. A. B. Blumenthal, H. J. Kriegstein, D. S. Hogness, *Cold Spring Harbor Symp. Quant. Biol.* **38**, 205 (1974); S. L. McKnight and O. L. Miller, *Cell* **12**, 795 (1977); V. A. Zakian, *J. Mol. Biol.* **108**, 305 (1976).
  20. R. T. Kamakaka, P. D. Kaufman, B. Stillman, P. G. Mitsis, J. T. Kadonaga, *Mol. Cell. Biol.* **14**, 5114 (1994); C. S. Chiang, P. G. Mitsis, I. R. Lehman, *Proc. Natl. Acad. Sci. U.S.A.* **90**, 9105 (1993).
  21. E. Harlow and D. Lane, Eds., *Antibodies* (Cold Spring Harbor Laboratory, Cold Spring Harbor, NY, 1988).
  22. Alignments were performed with the ClustalW program [J. D. Thompson, D. G. Higgins, T. J. Gibson, *Nucleic Acids Res.* **22**, 4673 (1994)].
  23. Fraction number variation among different glycerol gradients (23 fractions for the molecular mass stan-

dards, 20 fractions for recombinant DmORC2, and 21 fractions for the complex) was corrected by normalization of each fraction to  $V/V_i$  (the ratio of cumulative eluted volume to total gradient volume). The leftmost and rightmost lanes of each protein immunoblot and silver stain correspond to fractions eluted at 36% and 79% of the total volume, respectively.

24. We thank C. Zuker for providing the *DmORC2* genomic clone, D. Rio for bringing the initial finding of the Zuker lab to our attention, M. Levine (University of California, San Diego) for the plasmid cDNA library, T. Kornberg for the  $\lambda$ gt10 cDNA library, D. Rio and R. Tjian for encouragement and technical advice, and A. Ho for help. Supported by a pilot project grant from the National Institute of Environmental Health Sciences Mutagenesis Center (ES-01896), National Cancer Institute grant CA30490, and a Human Frontier Science Program Long-Term Research Fellowship (M.G.). Sequences of the *DmORC2* and *DmORC5* cDNAs have been deposited in GenBank (accession numbers pending).

6 October 1995; accepted 13 November 1995

## Early-Onset Epilepsy and Postnatal Lethality Associated with an Editing-Deficient *GluR-B* Allele in Mice

Rossella Brusa, Frank Zimmermann, Duk-Su Koh, Dirk Feldmeyer, Peter Gass, Peter H. Seeburg, Rolf Sprengel

The arginine residue at position 586 of the *GluR-B* subunit renders heteromeric  $\alpha$ -amino-3-hydroxy-5-methyl-4-isoxazolepropionate (AMPA)-sensitive glutamate receptor channels impermeable to calcium. The codon for this arginine is introduced at the precursor messenger RNA (pre-mRNA) stage by site-selective adenosine editing of a glutamine codon. Heterozygous mice engineered by gene targeting to harbor an editing-incompetent *GluR-B* allele synthesized unedited *GluR-B* subunits and, in principal neurons and interneurons, expressed AMPA receptors with increased calcium permeability. These mice developed seizures and died by 3 weeks of age, showing that *GluR-B* pre-mRNA editing is essential for brain function.

Glutamate receptors sensitive to AMPA are ligand-activated cation channels that mediate the fast component of excitatory postsynaptic currents in central neurons (1). These channels are assembled from four related subunits (*GluR-A* to *GluR-D*, or *GluR1* to *GluR4*) (2), with the *GluR-B* subunit rendering the channel almost impermeable to Ca<sup>2+</sup> (3). The molecular determinant for this dominant property of *GluR-B* was traced to the arginine (R) residue at position 586 of the mature subunit, which lies within the pore-forming segment M2 (4). This arginine is not gene encoded (5) but is posttranscriptionally introduced

into *GluR-B* pre-mRNA (5, 6) by site-selective adenosine deamination, which leads to the change of a CAA glutamine (Q) codon to a CIG codon for arginine in >99% of mRNA molecules (5–7). Termed Q/R site editing, this nuclear process depends on a double-stranded RNA structure (6) formed in the pre-mRNA by the editing site in exon 11 and the editing site complementary sequence (ECS) in intron 11 (8). To investigate in an animal model the relevance of this process for central nervous system (CNS) physiology, we targeted intron 11 of the *GluR-B* gene in mouse embryonic stem (ES) cells (9) for replacement of the ECS element (10) by *loxP* (11, 12) (Fig. 1), and then injected correctly engineered cells into C57BL/6 blastocysts. One of several resultant chimeric animals showed vertical transmission of the *GluR-B* <sup>$\Delta$ ECS</sup> allele in a Mendelian fashion (10), indicating that the allele did not adversely affect embryonic development.

In brains of *GluR-B* <sup>$\Delta$ ECS</sup> mice, the

*GluR-B* <sup>$\Delta$ ECS</sup> allele was expressed with its transcripts remaining unedited at the Q/R site, demonstrated by analysis of allele-specific reverse transcription-polymerase chain reaction (RT-PCR) products (13) of partially spliced *GluR-B* pre-mRNA (Fig. 2A). The sequence and hybridization analysis of RT-PCR products revealed that pre-mRNA derived from the wild-type allele was edited to the expected extent of 83% (6, 13), whereas pre-mRNA from the *GluR-B* <sup>$\Delta$ ECS</sup> allele, in which the ECS element was replaced by *loxP*, was not edited at the Q/R site. These data showed that the ECS element is indispensable for Q/R site editing in vivo, as previously established for in vitro editing (6, 7). The RT-PCR analysis further indicated that *GluR-B* <sup>$\Delta$ ECS</sup> pre-mRNA sequences were amplified more efficiently than *GluR-B*<sup>+</sup> pre-mRNA (Fig. 2A). Quantification with primers that amplify DNA fragments of identical size for both allelic pre-mRNAs (13) revealed that premature transcripts of the *GluR-B* <sup>$\Delta$ ECS</sup> allele are enriched approximately fivefold in the nucleus as compared with premature transcripts of the *GluR-B*<sup>+</sup> allele. The nuclear accumulation of *GluR-B* <sup>$\Delta$ ECS</sup> pre-mRNA was attributable to a reduced splicing efficiency of the sequence-modified intron 11, because ribonuclease (RNase) protection with a suitable intron probe (14) revealed increased amounts of the *loxP*-containing intron 11 relative to the unmodified intron (Fig. 2B). Consequently, the amounts of cytoplasmic mRNA corresponding to the two alleles were imbalanced, with mature cytoplasmic transcripts unedited at the Q/R site constituting only 25  $\pm$  3% (mean  $\pm$  SEM,  $n = 8$ ), rather than the theoretically expected 50%, of the *GluR-B* mRNA population. This situation reflects an overall decrease in *GluR-B* mRNA abundance, and, indeed, a reduction of  $\sim$ 30% in the amount of *GluR-B* mRNA was demonstrated by densitometric analysis of Northern

R. Brusa, F. Zimmermann, P. H. Seeburg, R. Sprengel, Laboratory of Molecular Neuroendocrinology, Center for Molecular Biology (ZMBH), University of Heidelberg, Im Neuenheimer Feld 282, D-69120 Heidelberg, Germany. D.-S. Koh, D. Feldmeyer, B. Sakmann, Max-Planck-Institut für Medizinische Forschung, Abteilung Zellphysiologie, Jahnstrasse 29, D-69120 Heidelberg, Germany. P. Gass, Institut für Neuropathologie, University of Heidelberg, Im Neuenheimer Feld 220, D-69120 Heidelberg, Germany.

(RNA) blots (15) (Fig. 2C). Other than the imbalance in the mRNAs corresponding to the two alleles, *GluR-B* gene expression appeared normal by Northern analysis, RT-PCR, and in situ hybridization (Fig. 2D). The mutant mRNA was characterized (13) by the same flip-flop splice ratios (16) and extent of R/G site editing (17) as were wild-type transcripts, and the distribution of *GluR-B* mRNA in the brain was as expected (18). In summary, the abundance of *GluR-B* mRNA in *GluR-B*<sup>+/ $\Delta$ ECS</sup> mice is 70% of that in their wild-type littermates, and one-quarter of these transcripts are unedited at the Q/R site.

In *GluR-B*<sup>+/ $\Delta$ ECS</sup> mice, the functional hemizyosity with regard to Q/R site editing would be expected to result in a shortage of the edited *GluR-B* subunit for assembly of heteromeric AMPA receptors and, hence, an increase in the glutamate-activated Ca<sup>2+</sup> permeability of and Ca<sup>2+</sup> influx through these channels (19, 20). This prediction was confirmed by measurement of responses to fast application of glutamate in nucleated patches isolated from the soma of different neuronal cell types in various brain regions (21). For example, in hippocampal pyramidal neurons of the CA1 subfield, the shift of the current reversal potential in a solution containing a high (30 mM) Ca<sup>2+</sup> concentration to less negative potentials demonstrated that the Ca<sup>2+</sup> permeability of AMPA receptors in *GluR-B*<sup>+/ $\Delta$ ECS</sup> heterozygotes was 7.3 times that in wild-type homozygotes (Fig. 3). In two other types of principal neurons, cerebellar Purkinje cells and neocortical pyramidal cells, the Ca<sup>2+</sup> permeability of AMPA receptors in *GluR-B*<sup>+/ $\Delta$ ECS</sup> mice was also increased by a factor of 5.2 to 7.3 (Fig. 3B). Inhibitory basket cells of the dentate gyrus (DG) in *GluR-B*<sup>+/ $\Delta$ ECS</sup> mice showed an average Ca<sup>2+</sup>/Ca<sup>+</sup> permeability ratio of 1.2, which is somewhat smaller than that previously estimated from outside-out patch recordings (22). This difference is probably attributable to the presence of two classes of basket cells, one of which expresses AMPA receptors with a low Ca<sup>2+</sup> permeability that give rise to only small ensemble currents (Fig. 3B). These currents could be detected in nucleated patches but not in smaller outside-out patches. Basket cells with lower and higher AMPA receptor-mediated Ca<sup>2+</sup> permeability occurred also in *GluR-B*<sup>+/ $\Delta$ ECS</sup> mice, in which both groups of cells showed increased Ca<sup>2+</sup> permeabilities. The difference between the two groups was, however, less pronounced than in *GluR-B*<sup>+/ $\Delta$ ECS</sup> animals (Fig. 3B). Thus, if *GluR-B* expression is low, as in one class of DG basket cells, the Q/R site-edited subunit would contribute relatively little to the Ca<sup>2+</sup> permeability of AMPA receptors, and, on average, the increased permeability in the heterozygotes was therefore not as pronounced.

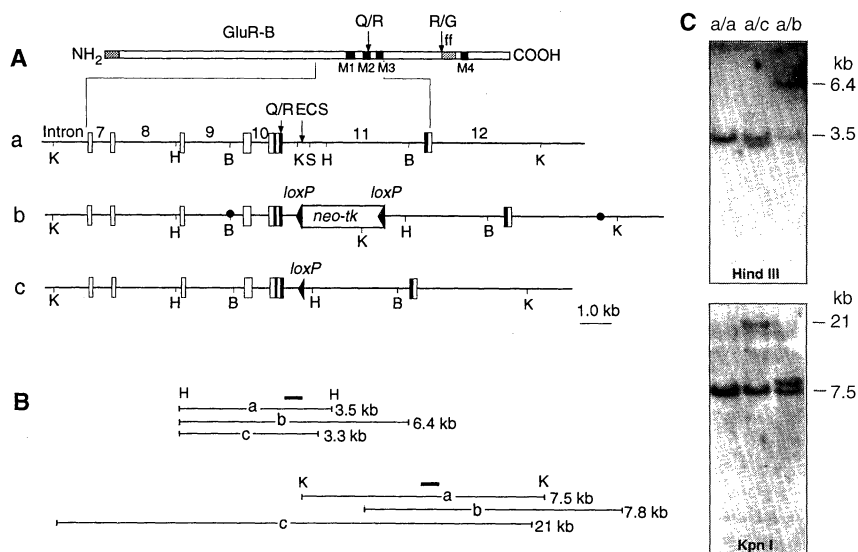
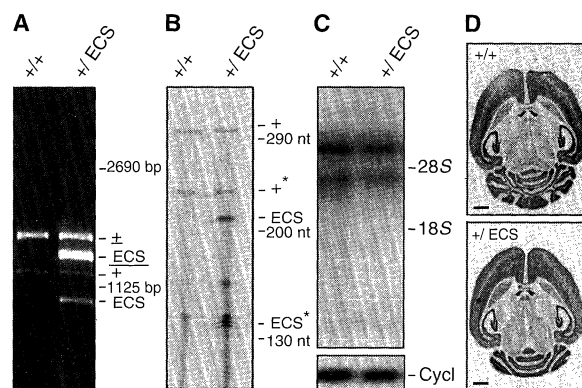


**Fig. 1.** Generation of *GluR-B*<sup>+/ $\Delta$ ECS</sup> mice. **(A)** Schematic representation of the *GluR-B* subunit and of gene segments (8) of the wild-type *GluR-B*<sup>+</sup> allele (a), the targeted *GluR-B*<sup>neo</sup> allele (b), and the *GluR-B* <sup>$\Delta$ ECS</sup> allele after Cre recombination (c) (10). For the protein, Q/R and R/G editing sites (5, 6, 17) are indicated by arrows; black boxes represent putative membrane segments M1 to M4 (2); the hatched box shows the position of the alternatively spliced flip-flop exons (ff) (16); and the gray box represents the signal peptide. For the gene segments, open boxes represent exonic sequences (8). The *loxP* sites are shown by triangles and the *neo-tk* cassette by an open box. The solid circles in segment b delineate the 5' and 3' ends of the targeting construct. Relevant restriction enzyme recognition sites are indicated: K, Kpn I; B, BsrG I; S, Sca I; H, Hind III. **(B and C)** Genomic Hind III (H) and Kpn I (K) restriction fragments (B) used in Southern blot analysis (C) to distinguish the *GluR-B* alleles a, b, and c in targeted R1 ES cell clones. Southern probes and their positions (10) are indicated by black bars in (B).

**Fig. 2.** *GluR-B* transcript analysis. RNA from the brains of *GluR-B*<sup>+/ $\Delta$ ECS</sup> and *GluR-B*<sup>+/ $\Delta$ ECS</sup> mice was analyzed by various techniques. **(A)** RT-PCR analysis with exon-10 and intron-11 primers (13). Amplified fragments containing intron 10 and derived from pre-mRNA or gene sequences are indicated according to allele type by underlined symbols. Amplicons lacking intron 10 and derived from pre-mRNA are denoted by allele symbols that are not underlined, and were cloned for analysis of pre-mRNA. **(B)** RNase protection analysis (14). Probe segments protected by the intron-11 sequence in the pre-mRNAs derived from *GluR-B*<sup>+</sup> and *GluR-B* <sup>$\Delta$ ECS</sup> alleles are indicated by allele symbols (+,  $\Delta$ ECS). An asterisk indicates probe segments identified as degradation products resulting from overdigestion. Self-protected probe fragments with lower signal intensity are not indicated. **(C)** Northern blot analysis (15) with the RNA load controlled for by reprobing the membrane with a probe for cyclophilin mRNA (Cycl). The positions of 28S and 18S ribosomal RNAs are indicated. **(D)** In situ hybridization of *GluR-B* mRNA from brains of *GluR-B*<sup>+/ $\Delta$ ECS</sup> (upper panel) and *GluR-B*<sup>+/ $\Delta$ ECS</sup> (lower panel) mice (18). Scale bar, 1 mm.



Molecular differences between the *GluR-B*<sup>+/ $\Delta$ ECS</sup> and *GluR-B*<sup>+/ $\Delta$ ECS</sup> animals were revealed in the expression of the Ca<sup>2+</sup>-responsive immediate-early genes *c-Fos*, *c-Jun*, and *Krox24* (23), which likely result from the increased glutamate-activated Ca<sup>2+</sup> entry into the neurons of heterozygous animals. As observed by in situ hybridization, the abundance of *c-Jun* and *Krox24* (24) mRNAs was consistently increased in

several brain areas of *GluR-B*<sup>+/ $\Delta$ ECS</sup> mice (Fig. 4A). In particular, *c-Jun* expression was increased in CA1 pyramidal neurons, whereas *Krox24* expression was increased in CA3 pyramidal neurons. Changes in *c-Fos* expression differed among individual heterozygotes, perhaps reflecting the occurrence of spontaneous seizures (see below). In contrast, the abundance of transcripts for AMPA and N-methyl-D-aspartate receptor

**Fig. 3.** Relative  $\text{Ca}^{2+}$  permeability of AMPA receptors in neurons of  $\text{GluR-B}^{+/+}$  and  $\text{GluR-B}^{+/\Delta\text{ECS}}$  mice. (A) Left panels: AMPA receptor-mediated currents in hippocampal CA1 pyramidal cells evoked by 100-ms pulses of 1 mM glutamate in high- $\text{Na}^+$  and high- $\text{Ca}^{2+}$  extracellular solutions, as indicated. The membrane potential was varied between  $-80$  and  $80$  mV in  $20$ -mV steps. Right panels: Corresponding peak current-voltage ( $I$ - $V$ ) relations for high- $\text{Na}^+$  (○) and high- $\text{Ca}^{2+}$  (●) solutions. Arrows indicate the reversal potential in high- $\text{Ca}^{2+}$  solution. The  $I$ - $V$  relations were fitted by third- to sixth-order polynomials, from which the interpolated reversal potentials were calculated. (B) Left panel:  $\text{Ca}^{2+}$  permeability of AMPA receptors in four classes of neurons in  $\text{GluR-B}^{+/+}$  and  $\text{GluR-B}^{+/\Delta\text{ECS}}$  mice. Relative  $\text{Ca}^{2+}$  permeability, expressed as the ratio of  $\text{Ca}^{2+}$  permeability to  $\text{Na}^+$  permeability ( $P_{\text{Ca}}/P_{\text{Na}}$ ), is plotted for  $\text{GluR-B}^{+/+}$  (open columns) and  $\text{GluR-B}^{+/\Delta\text{ECS}}$  (filled columns) mice. Values are means  $\pm$  SD of 27 experiments with eight  $\text{GluR-B}^{+/+}$  mice and 46 experiments with seven  $\text{GluR-B}^{+/\Delta\text{ECS}}$  mice. Right panels: Plots of relative  $\text{Ca}^{2+}$  permeability against peak current size at  $-40$  mV in DG basket cells of  $\text{GluR-B}^{+/+}$  and  $\text{GluR-B}^{+/\Delta\text{ECS}}$  mice as indicated.

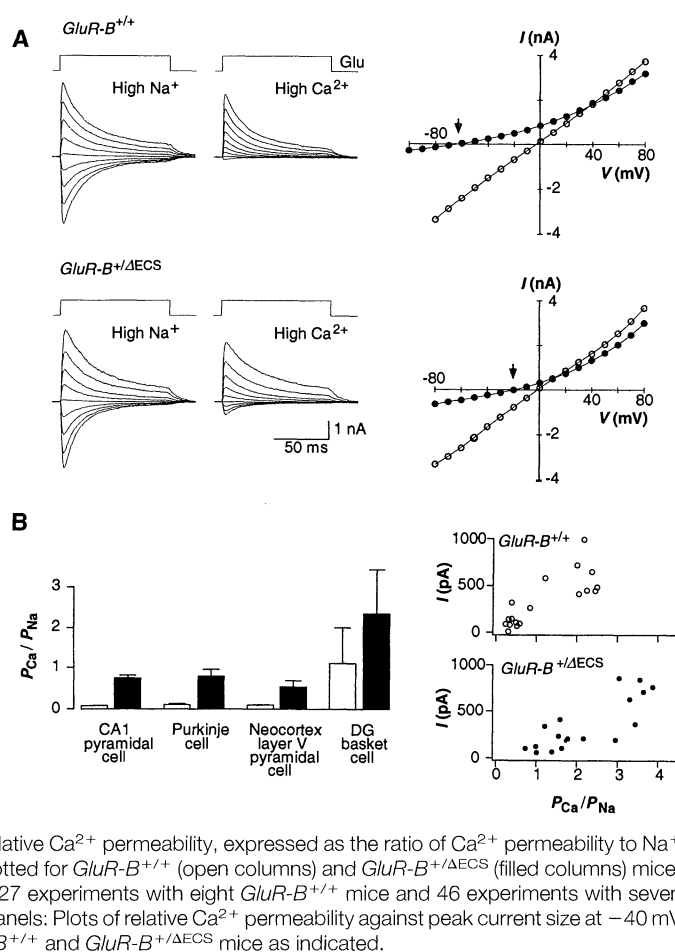
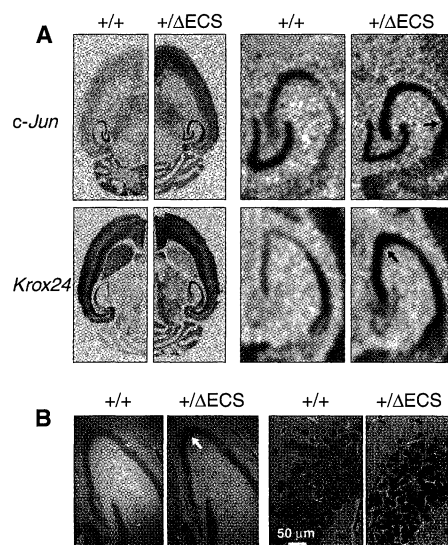


**Fig. 4.** Histological analysis of brains from  $\text{GluR-B}^{+/+}$  and  $\text{GluR-B}^{+/\Delta\text{ECS}}$  mice. (A) Autoradiograms of horizontal brain sections (P15) hybridized with  $^{35}\text{S}$ -labeled oligonucleotides specific for *c-Jun* and *Krox24* mRNAs (24). Half-brain images from wild-type ( $+/+$ ) and heterozygous ( $+/\Delta\text{ECS}$ ) mice were apposed to permit better evaluation of expression differences. The hippocampal regions are shown enlarged on the right. Arrows point to the CA3 field for *Krox24* and to the CA1 field for *c-Jun*. (B) Hippocampal sections from mouse brains ( $15 \mu\text{m}$ ), fixed by immersion in 4% paraformaldehyde and embedded in paraffin, were stained with hematoxylin-eosin. The close-ups on the right show the CA3 layer and reveal an increased abundance of eosinophilic cells in the  $\text{GluR-B}^{+/\Delta\text{ECS}}$  brain. Arrow indicates the CA3 field.



subunits appeared unaltered (2, 16, 25). During the first two postnatal weeks, the heterozygous animals appeared healthy except for an incipient hypotrophy. Beginning at postnatal day 13 (P13), all carriers of the  $\text{GluR-B}^{\Delta\text{ECS}}$  allele rapidly developed a severely compromised phenotype, resulting from a neurological syndrome of which the most recognizable manifestations were spontaneous and recurrent seizures, as well as progressively agitated states with excessive jumping and running fits (26). All heterozygotes died by P20. Postmortem analysis of

the brains of three animals that underwent prolonged seizure episodes revealed selective neuronal degeneration in the lateral region of the hippocampal CA3 field, with  $\sim 50\%$  of the neurons showing shrunken nuclei and acidophilic cytoplasmic staining (27) (Fig. 4B). Neuronal degeneration was acute in the absence of glial reactions, as assessed by histology and by immunocytochemistry for

glial acidic fibrillary protein. Detailed analyses revealed no other apparent abnormalities in the central or peripheral nervous system, and skeletal muscles and visceral organs showed normal histology (27). Thus, aberrant excitatory signaling, rather than morphological changes, may underlie the compromised phenotype.

The dominant lethal effect of the  $\text{GluR-B}^{\Delta\text{ECS}}$  allele with a penetrance of 100% demonstrates that efficient Q/R site editing of  $\text{GluR-B}$  pre-mRNA (5, 16) and the resulting low  $\text{Ca}^{2+}$  permeability of AMPA receptors in excitatory principal neurons (19) are pivotal for CNS physiology. Our data suggest that the onset and severity of the epileptic phenotype engendered by a reduction of Q/R site editing depend on the ratio of edited to unedited  $\text{GluR-B}$  subunits (28). It is possible that epileptic mouse models related to altered AMPA receptor properties could be established by regulating this ratio. Indeed, the selective destruction of hippocampal neurons in  $\text{GluR-B}^{+/\Delta\text{ECS}}$  mice is reminiscent of kainate-induced hippocampal lesions, which are relevant to human temporal lobe epilepsy (29). It remains to be determined whether any of the human familial epilepsies (30) derive from related molecular defects.

REFERENCES AND NOTES

1. M. L. Mayer and G. L. Westbrook, *J. Physiol. (London)* **394**, 501 (1987); S. Hestrin, *Neuron* **11**, 1083 (1993); P. Jonas and N. Spruston, *Curr. Opin. Neurobiol.* **4**, 366 (1994).
2. M. Hollmann and S. Heinemann, *Annu. Rev. Neurosci.* **17**, 31 (1994).
3. M. Hollmann, M. Hartley, S. Heinemann, *Science* **252**, 852 (1991); T. A. Verdoorn, N. Burnashev, H. Monyer, P. H. Seeburg, B. Sakmann, *ibid.*, p. 1715.
4. R. I. Hume, R. Dingledine, S. F. Heinemann, *ibid.* **253**, 1028 (1991); N. Burnashev, H. Monyer, P. H. Seeburg, B. Sakmann, *Neuron* **8**, 189 (1992).
5. B. Sommer, M. Köhler, R. Sprengel, P. H. Seeburg, *Cell* **67**, 11 (1991).
6. M. Higuchi *et al.*, *ibid.* **75**, 1361 (1993).
7. T. Melcher, S. Maas, M. Higuchi, W. Keller, P. H. Seeburg, *J. Biol. Chem.* **270**, 8566 (1995); S. M. Rueter, C. M. Burns, S. A. Coode, P. Mookherjee, R. B. Emeson, *Science* **267**, 1491 (1995); J. H. Yang, P. Sklar, R. Axel, T. Maniatis, *Nature* **374**, 77 (1995).
8. M. Köhler, H. C. Kornau, P. H. Seeburg, *J. Biol. Chem.* **269**, 17367 (1994).
9. A. Nagy, J. Rossant, R. Nagy, N. W. Abramow, J. C. Roder, *Proc. Natl. Acad. Sci. U.S.A.* **90**, 8424 (1993).
10. For construction of the targeting vector pGRB-neotk-1, a BsrGI-SalI mouse 129/sv genomic fragment containing exons 9 to 12 of the *GluR-B* locus (8) was subcloned into pBluescript SK II(-) (Stratagene). The 358-base pair (bp) KpnI-ScaI genomic fragment of intron 11, which contains the ECS site, was deleted and replaced by a *loxP-neo<sup>r</sup>-tk-loxP* cassette from vector pneotk-1 (R. Sprengel, unpublished data). R1 ES cells (9) were electroporated (Bio-Rad Gene Pulser set at 240 V and 500  $\mu\text{F}$ ) with 40  $\mu\text{g}$  of pGRB-neotk-1 that had been linearized at the unique SalI site in the polylinker. Cell clones resistant to G418 (300  $\mu\text{g}/\text{ml}$ ) selection were isolated after 7 to 10 days. Four targeted clones were identified by nested PCR analysis with rsp27 (5'-AGGACGGCGGCAAAACGAGGGCACCCG-3') and rsp28 (5'-GCAGGCAAGAGCCGAGGCGGAGGCCAAG-3') as sense primers in intron-9 sequences

- outside of the targeting vector and rpsne6 (5'-GCAATCCATCTTGTTCATGGC-3') and rpslox5 (5'-CACTGCTCGACCTGACGCCAAG-3') as antisense primers of the *neo* cassette. Homologous recombination was confirmed by Southern (DNA) blot analysis (Fig. 1C). To delete the selection marker cassette,  $10^7$  *Glur-B<sup>+/neo</sup>* ES cells were electroporated with 30  $\mu$ g of Cre-encoding plasmid, pMC-Cre (12). After 5 to 7 days of ganciclovir (2  $\mu$ M) selection, the resistant clones were picked and analyzed by PCR with a primer set [sense primer MH53 (5'-GTGATCATGTGTTCCCTG-3') located in intron 11 upstream of the Kpn I site (6), and antisense primer rsp36 (5'-CAATAGCAATTGGTGATTTGTGAC-3') located in intron 11, 3' of the Sca I site] that amplified a 494-bp fragment of the *Glur-B<sup>+</sup>* and a 250-bp fragment of the *Glur-B<sup>ΔECS</sup>* allele. Genotypes of *Glur-B<sup>+/ΔECS</sup>* clones were confirmed on Southern blots (Fig. 1C) of Hind III-digested DNA probed with a 400-bp Bgl II-Kpn I fragment derived from exon-11 and intron-11 sequences, or of Kpn I-digested DNA probed with an 800-bp Bgl II-Hpa I fragment encompassing the 3' portion of intron 11 and exon 12 (8). The absence of *neo* [E. Beck et al., *Gene* **19**, 327 (1982)] and *cre* sequences (17) in the genome of the clones was confirmed by PCR. Three independent targeted clones that contained the correct sequence replacement were injected into blastocysts of C57BL/6 mice. Of several male chimeras, only one, derived from clone GRB1/50/Cre/13, transmitted the mutated *Glur-B* allele to offspring, whose genotype was determined from tail DNA by PCR analysis with primers MH53 and rsp36 and by Southern hybridization. Of 89 agouti offspring, 43 were *Glur-B<sup>+/ΔECS</sup>*.
- N. Sternberg, B. Sauer, R. Hoess, K. Abremski, *J. Mol. Biol.* **187**, 197 (1986).
  - H. Gu, Y. R. Zou, K. Rajewsky, *Cell* **73**, 1155 (1993).
  - RT-PCR amplification of *Glur-B* pre-mRNA sequences from brain tissue [three *Glur-B<sup>+/+</sup>* animals and six *Glur-B<sup>+/ΔECS</sup>* animals, all P15 to P18] was performed with sense primer rspx10a (5'-GCGGATCCGGAAATGAGCGT TACGAGGGCTAC-3', exon 10) and antisense primer rsp36b (5'-CCAATG-CATTTGTGACAAATACTGATAATTAG-3', intron 11) or, for quantitative studies, MH36 (5'-TCAC-CAGGGAAACACATGATC-3', intron 11). For mRNA analysis, amplification primers B52 (7) and 3'lamlo [B. Lambalez, E. Audinat, B. Bochet, F. Crepel, J. Rossier, *Neuron* **9**, 247 (1992)], which are derived from exons 11 and 14-15 (8), respectively, were used. For analysis of posttranscriptional modifications, the amplicons (Fig. 2A) were directionally cloned into M13mp19 replicative form DNA and recombinant plaques were analyzed by differential oligonucleotide hybridization (5, 6, 16, 17) for Q/R site editing in partially spliced pre-mRNA and mRNA, and for ratios of flip-flop splice forms and of R/G site editing in mRNA. Pre-mRNA was analyzed either from RT-PCR products with primers rspx10a and rsp36b, which differ in size for the *Glur-B<sup>+</sup>* and *Glur-B<sup>ΔECS</sup>* transcripts and were cloned individually (allele-specific analysis; 17% Q form in *Glur-B<sup>+</sup>* pre-mRNA, 100% Q form in *Glur-B<sup>ΔECS</sup>* pre-mRNA), or from RT-PCR products with primers rspx10a and MH36, which are identical in size for the two alleles [17% Q form in *Glur-B<sup>+/+</sup>* mice; 88  $\pm$  3% (mean  $\pm$  SD,  $n$  = 3) Q form in *Glur-B<sup>+/ΔECS</sup>* mice]. The mRNA analysis (Q forms were assigned to mRNA from the *Glur-B<sup>ΔECS</sup>* allele and R forms to the *Glur-B<sup>+</sup>* allele) revealed 25  $\pm$  3% (mean  $\pm$  SEM,  $n$  = 8) Q form in *Glur-B<sup>+/ΔECS</sup>* mice and <1% Q form in *Glur-B<sup>+/+</sup>* mice; 50  $\pm$  1% (mean  $\pm$  SD,  $n$  = 3) flip in both *Glur-B<sup>ΔECS</sup>* mRNA and *Glur-B<sup>+</sup>* mRNA; 71  $\pm$  2% flip R form and 68  $\pm$  5% flop R form in *Glur-B<sup>ΔECS</sup>* mRNA; and 88  $\pm$  2% flip G form and 76  $\pm$  6% flop G form in *Glur-B<sup>+</sup>* mRNA.
  - For RNase protection analysis [J. M. Ausubel et al., Eds., *Current Protocols in Molecular Biology* (Wiley Interscience, New York, 1994)], a 315-bp Eco RI-Hinc II fragment from intron 11 of the murine *Glur-B* gene (8) was cloned in pBluescript II SK(-). The resulting plasmid was linearized at the Xba I site in the polylinker, and antisense RNA was generated by in vitro transcription with T7 polymerase in the presence of [ $\alpha$ - $^{32}$ P]uridine 5'-triphosphate. The  $^{32}$ P-labeled riboprobe [369 nucleotides (nt)] was hybridized to 20  $\mu$ g of total brain RNA from wild-type and mutant mice and then incubated with RNases A (20  $\mu$ g/ml) and T1 (1  $\mu$ g/ml). The major protected RNA fragments were resolved on a 6% polyacrylamide gel and visualized by autoradiography (2 to 6 days of exposure). The sizes of the protected fragments were 316 nt for the *Glur-B<sup>+</sup>* and 217 nt for the *Glur-B<sup>ΔECS</sup>* transcripts. Quantification of the protected fragments by densitometric analysis (MacBAS software, Fuji) revealed a three- to fivefold increase in mutant transcripts relative to wild-type transcripts containing intron 11.
  - Glur-B*-specific signals on Northern blots of brain RNA from *Glur-B<sup>+/ΔECS</sup>* and *Glur-B<sup>+/+</sup>* animals (P15) obtained with a 350-bp probe (Eco RI, complementary DNA positions 2583 to 2949) derived from the 3' untranslated region (8) were normalized to cyclophilin mRNA [P. E. Danielson et al., *DNA* **7**, 261 (1988)] and quantitatively assessed by densitometry (Fuji Bas 3000). The average relative signal difference between wild-type ( $n$  = 2) and heterozygous ( $n$  = 10) mice was 30  $\pm$  9% (mean  $\pm$  SD).
  - B. Sommer et al., *Science* **249**, 1580 (1990).
  - H. Lomeli et al., *ibid.* **266**, 1709 (1994).
  - K. Keinänen et al., *ibid.* **249**, 556 (1990); K. Sakimura et al., *FEBS Lett.* **272**, 73 (1990).
  - P. Jonas, C. Racca, B. Sakmann, P. H. Seeburg, H. Monyer, *Neuron* **12**, 1281 (1994); J. R. P. Geiger et al., *ibid.* **15**, 193 (1995).
  - N. Burnashev, Z. Zhou, E. Neher, B. Sakmann, *J. Physiol. (London)* **485**, 403 (1995).
  - Transverse hippocampal and neocortical slices or parasagittal cerebellar slices with a thickness of 300  $\mu$ m were cut from the brains of eight *Glur-B<sup>+/+</sup>* and seven *Glur-B<sup>+/ΔECS</sup>* mice (P14 to P19). Cells were identified visually by infrared differential interference contrast video microscopy [G. J. Stuart, H.-U. Dodt, B. Sakmann, *Pflügers Arch.* **423**, 511 (1993)]. DG basket cells were also identified by their location at the hilar border of the DG, the triangular shape of their soma, and their discharge pattern (19). To increase the size of currents mediated by AMPA receptors, we performed electrophysiological experiments with nucleated patches [W. Sather, S. Dieu-donné, J. F. MacDonald, P. Ascher, *J. Physiol. (London)* **450**, 643 (1992)] that had diameters of 7 to 12  $\mu$ m. In some experiments with cerebellar Purkinje cells, outside-out patches were used. Slices were continuously superfused with physiological extracellular saline solution, containing 125 mM NaCl, 25 mM NaHCO<sub>3</sub>, 25 mM glucose, 2.5 mM KCl, 1.25 mM NaH<sub>2</sub>PO<sub>4</sub>, 2 mM CaCl<sub>2</sub>, and 1 mM MgCl<sub>2</sub>, that was bubbled with 95% O<sub>2</sub> and 5% CO<sub>2</sub>. A Hepes-buffered high-Na<sup>+</sup> extracellular solution, used for perfusing the application pipette, contained 135 mM NaCl, 5.4 mM KCl, 1.8 mM CaCl<sub>2</sub>, 1 mM MgCl<sub>2</sub>, and 5 mM Hepes-NaOH (pH 7.2). The high-Ca<sup>2+</sup> extracellular solution contained 30 mM CaCl<sub>2</sub>, 105 mM *N*-methyl-D-glucamine, and 5 mM Hepes-HCl (pH 7.2). D-2-Amino-5-phosphonovaleric acid (25  $\mu$ M) was added to block *N*-methyl-D-aspartate receptor channels. The high-Cs<sup>+</sup> intracellular solution contained 140 mM CsCl, 10 mM EGTA, 2 mM MgCl<sub>2</sub>, 2 mM adenosine triphosphate (disodium salt), and 10 mM Hepes-CsOH (pH 7.3). The  $P_{Ca}/P_{Na}$  values were determined from the reversal potentials in Na<sup>+</sup>-rich extracellular solution ( $V_{revNa}$ ) and Ca<sup>2+</sup>-rich extracellular solution ( $V_{revCa}$ ) according to the following equation:
$$P_{Ca}/P_{Na} = 0.25 a_{Na}/a_{Ca} [\exp(2V_{revCa} - V_{revNa})/F/RT] + \exp[(V_{revCa} - V_{revNa})/F/RT]$$
where  $a_{Na}$  and  $a_{Ca}$  are the activities of Na<sup>+</sup> and Ca<sup>2+</sup> in the extracellular solutions, respectively, and  $R$ ,  $T$ , and  $F$  have their conventional meaning [C. A. Lewis, *J. Physiol. (London)* **286**, 417 (1979)]. Activity coefficients were estimated by interpolation of tabulated values (0.75 for NaCl, 0.55 for CaCl<sub>2</sub>). Both  $V_{revCa}$  and  $V_{revNa}$  values were corrected for liquid junction potentials of 9.8 and 4.5 mV, respectively.
  - D.-S. Koh, J. R. P. Geiger, P. Jonas, B. Sakmann, *J. Physiol. (London)* **485**, 383 (1995).
  - J. I. Morgan and T. Curran, *Annu. Rev. Neurosci.* **14**, 421 (1991); P. Gass, T. Herdegen, R. Bravo, M. Kiessling, *Neuroscience* **48**, 315 (1992); W. J. Gallin and M. E. Greenberg, *Curr. Opin. Neurobiol.* **5**, 367 (1995).
  - W. Wisden et al., *Neuron* **4**, 603 (1990).
  - M. Watanabe, Y. Inoue, K. Sakimura, M. Mishina, *Neuroreport* **3**, 1138 (1992); T. Ishii et al., *J. Biol. Chem.* **268**, 2836 (1993); H. Monyer, N. Burnashev, D. J. Laurie, B. Sakmann, P. H. Seeburg, *Neuron* **12**, 529 (1992).
  - All heterozygotes developed overt behavioral seizures [R. J. Racine, *Electroencephalogr. Clin. Neurophysiol.* **32**, 281 (1972)]. A total of 14 heterozygous and 10 wild-type mice were observed from P12 for various time periods (8 to 12 hours), and representative video recordings were made. At P13 to P14, all heterozygotes, but none of the wild-type mice, developed recurrent seizures with a "behavioral" similar to that of kainic acid-induced limbic seizures [J. V. Nadler, *Life Sci.* **29**, 2031 (1981)], characterized by rearing on hindlimbs and concomitant forelimb tremor. In addition to these limbic seizure episodes, animals showed spontaneous tonic-clonic seizures (persisting for 20 to 60 s) followed by drowsiness and altered states of consciousness. On average, generalized seizures occurred two to three times during observation periods. These seizures alternated with jumping and running fits over periods of 2 to 3 hours, and persisted for ~2 days. In the subsequent days (P16 to P20), the heterozygous mice developed a severely compromised phenotype characterized by growth retardation, weakness of the hindlimbs, progressively agitated states with chewing-grooming automatism, excessive jumping and running fits, and, finally, stupor and death.
  - For histological analyses [B. D. Distrey and J. H. Rack, *Histological Laboratory Methods* (E. & S. Publishers, Edinburgh, U.K., 1970)], two heterozygous and two wild-type mice were perfused transcardially with 4% paraformaldehyde at ages P15, P17, P18, and P19. Brain and visceral organs were dissected, embedded in paraffin, and analyzed as 1- $\mu$ m sections. Apart from hypotrophy of all organ systems, no gross abnormalities were evident in the central or peripheral nervous system, skeletal muscles, or visceral organs of heterozygotes. In the CNS, all major neuronal populations were present and did not show histological abnormalities, as judged by light microscopic examination of serial sections (1- $\mu$ m coronal sections every 100  $\mu$ m) treated with Nissl's stain or hematoxylin-eosin. The cortex of the telencephalon and cerebellum exhibited regular layering. Myelination was also equal in mutant and wild-type animals, as assessed by histochemistry (Küver-Barrera staining) and immunocytochemistry for myelin basic protein. Marker molecules for specific neuronal subpopulations, including tyrosine hydroxylase, glutamate decarboxylase, parvalbumin, and calbindin [K. D. Beck, L. Powell-Braxton, H. R. Widmer, J. Valverde, F. Hefti, *Neuron* **14**, 717 (1995)], showed the same distribution and were detected in similar numbers of neurons in mutant and wild-type animals. Equal numbers of astrocytes expressing glial fibrillary acidic protein were observed in wild-type and mutant mice, and these cells were particularly abundant in the hippocampus and along white matter tracts.
  - Two chimeric founders derived from the targeted cell line containing the *neo* cassette in intron 11 (Fig. 1A, allele b) gave rise to *Glur-B<sup>+/neo</sup>* offspring. *Glur-B<sup>+/neo</sup>* mice had a ratio of Q/R site-edited to unedited *Glur-B* mRNA of 10:1 ( $n$  = 2), and of 14 heterozygotes only 2 died of seizure-related causes around P30.
  - S. Nakajima, J. E. Franck, D. Bilkey, R. A. Schwartzkroin, *Hippocampus* **1**, 67 (1991).
  - W. A. Hauser and D. C. Heschdorfer, *Epilepsy: Frequency, Causes, and Consequences* (Demos, New York, 1990); J. O. McNamara, *J. Neurosci.* **14**, 3413 (1994).
  - We thank B. Sakmann and M. Kiessling for their interest and support; I. Schiller and H. Monyer for critical discussions; M. Higuchi for advice and materials; A. Nagy for the R1 ES cell line; H. Gu for the plasmids pGEM-30, pGH-1, and pMC-Cre; A. Herold for DNA sequencing; U. Amtman for help with in situ hybridization; and R. Pfeiffer for animal care. R.B. was the recipient of a doctoral fellowship from the University of Torino, Italy. Supported, in part, by Sonderforschungsbereich grant 317 and funds from the German Chemical Society to P.H.S.

14 September 1995; accepted 24 October 1995

29. Streit, A. & Stern, C. D. Mesoderm patterning and somite formation during node regression: differential effects of chordin and noggin. *Mech. Dev.* **85**, 85–96 (1999).  
 30. Stern, C. D. Detection of multiple gene products simultaneously by *in situ* hybridization and immunohistochemistry in whole mounts of avian embryos. *Curr. Top. Dev. Biol.* **36**, 223–243 (1998).

**Acknowledgements**

We thank A. Rosenthal and W. Ye (Genentech) for the FGFR1-IgG construct; R. Lovell-Badge for *Sox3* and *Sox2* and T. Jessell for S17; C. Dulac for advice on the differential screen; B. Cigich for technical assistance; I. Skromne for Fig. 4b, c; C. Ang for zebrafinch tissue; and T. Jessell, G. Sheng, K. Storey and D. Vasiliaskas for helpful comments on the manuscript. Supported by the National Institute of Mental Health.

Correspondence and requests for materials should be addressed to C.D.S. (e-mail: cds20@columbia.edu).

**Point mutation in an AMPA receptor gene rescues lethality in mice deficient in the RNA-editing enzyme ADAR2**

Miyoko Higuchi\*, Stefan Maas\*†‡, Frank N. Single\*†, Jochen Hartner\*, Andrei Rozov§, Nail Burnashev§, Dirk Feldmeyer§, Rolf Sprengel\* & Peter H. Seeburg\*

\* Departments of Molecular Neurobiology and § Cell Physiology, Max-Planck Institute for Medical Research, Jahnstrasse 29, 69120 Heidelberg, Germany

† These authors contributed equally to this work

RNA editing by site-selective deamination of adenosine to inosine<sup>1,2</sup> alters codons<sup>3,4</sup> and splicing<sup>5</sup> in nuclear transcripts<sup>6</sup>, and therefore protein function. ADAR2 (refs 7, 8) is a candidate mammalian editing enzyme that is widely expressed in brain and other tissues<sup>7</sup>, but its RNA substrates are unknown. Here we have studied ADAR2-mediated RNA editing by generating mice that are homozygous for a targeted functional null allele. Editing in *ADAR2*<sup>-/-</sup> mice was substantially reduced at most of 25 positions in diverse transcripts<sup>3–6</sup>; the mutant mice became prone to seizures and died young. The impaired phenotype appeared to result entirely from a single underedited position, as it reverted to normal when both alleles for the underedited transcript were substituted with alleles encoding the edited version exonic<sup>9</sup>. The critical position specifies an ion channel determinant<sup>10</sup>, the Q/R site<sup>3,6</sup>, in AMPA (α-amino-3-hydroxy-5-methyl-4-isoxazole propionate) receptor<sup>10</sup> GluR-B pre-messenger RNA. We conclude that this transcript is the physiologically most important substrate of ADAR2.

Mammalian transcripts that are known to be edited by site-selective adenosine deamination are expressed largely in brain: most encode subunits of ionotropic glutamate receptors (GluRs) that mediate fast excitatory neurotransmission<sup>3,10</sup>. The only position edited to nearly 100% is the Q/R site of GluR-B, for which the mRNA contains an arginine (R) codon (CIG) in place of the genomic glutamine (Q) codon (CAG)<sup>3</sup>. The physiological importance of this codon substitution wrought by RNA editing was revealed by early onset epilepsy and premature death of mice heterozygous for an intron-11-modified *GluR-B*<sup>ΔECS</sup> allele with Q/R site-uneditable transcripts<sup>11,12</sup>.

Three mammalian adenosine deaminases acting on RNA

(ADAR1–ADAR3; refs 7, 8, 13) form a small family of candidate RNA-editing enzymes that operate on nuclear transcripts. Only ADAR2 edits the Q/R site in GluR-B pre-mRNA efficiently *in vitro*<sup>7,14,15</sup>. Because ADAR2 is expressed in tissues other than brain<sup>7</sup>, distinct pre-mRNAs in different tissues may be substrates for this enzyme. To determine whether ADAR2 edits the Q/R site in GluR-B pre-mRNA *in vivo*, and to evaluate the general physiological significance of ADAR2-mediated RNA editing, we generated mice with functional null alleles for this enzyme.

A targeting vector for functional *ADAR2* gene ablation (Fig. 1a, b) was constructed by replacing most of exon 4 (ref. 16) with a *PGK-neo* gene; exon 4 encodes an essential adenosine deaminase motif<sup>3,7</sup>. Chimaeric mice were generated by injection of a targeted embryonic stem (ES) cell clone<sup>17</sup> into C57BL/6-derived blastocysts. *ADAR2*<sup>+/-</sup> intercrosses produced *ADAR2*<sup>-/-</sup> mice at Mendelian frequency, indicating that ADAR2 deficiency does not interfere with embryonic development. We found residual expression from the targeted *ADAR2*<sup>-</sup> allele through exon skipping, potentially leading to a truncated, enzymatically inactive ADAR2 form with intact RNA-binding domains (Fig. 1c). The expression of this truncated form might amount to less than 10% of ADAR2 in wild-type mice, as predicted from the severely reduced mutant transcript levels (mean ± s.d., 8 ± 3% of wild type, *n* = 3; postnatal day 14 (P14)) determined by ribonuclease (RNase) protection (Fig. 1d).

Heterozygous *ADAR2*<sup>+/-</sup> mice were phenotypically normal, but *ADAR2*<sup>-/-</sup> mice died between P0 and P20 and became progressively seizure-prone after P12, akin to *GluR-B*<sup>+ΔECS</sup> mice<sup>11,12</sup>. Thus, we first studied the effect of ADAR2 deficiency on Q/R site editing of GluR-B pre-mRNA, the substrate for a nuclear RNA-dependent

**Table 1 ADAR2 deficiency and site-selective adenosine deamination**

| Editing sites   | ADAR2 <sup>+/+</sup> | ADAR2 <sup>+/-</sup> | ADAR2 <sup>-/-</sup> |
|-----------------|----------------------|----------------------|----------------------|
| GluR-B pre-mRNA |                      |                      |                      |
| Q/R*            | 98 ± 3               | 90 ± 3               | 10 ± 3               |
| Hotspot1*†      | 50                   | 45                   | 60                   |
| Hotspot2*†‡     |                      |                      |                      |
| +262            | 30                   | 20                   | <10                  |
| +263            | 65                   | 55                   | <10                  |
| +264            | 15                   | 10                   | <5                   |
| GluR-B mRNA     |                      |                      |                      |
| Q/R*            | 100 ± 1              | 100 ± 1              | 40 ± 4               |
| AMPA-R† R/G§    |                      |                      |                      |
| GluR-B          | 75                   | 55                   | 15                   |
| GluR-C          | 90                   | 85                   | 75                   |
| GluR-D          | 45                   | 40                   | 10                   |
| GluR5           |                      |                      |                      |
| Q/R             | 64 ± 5               | 55 ± 2               | 40 ± 1               |
| GluR6           |                      |                      |                      |
| Q/R             | 86 ± 4               | 78 ± 4               | 29 ± 8               |
| I/V             | 87 ± 2               | 79 ± 7               | 22 ± 5               |
| Y/C             | 90 ± 4               | 82 ± 5               | 2 ± 1                |
| 5HT2C-R†        |                      |                      |                      |
| A               | 75                   | 70                   | 70                   |
| B               | 80                   | 75                   | 30                   |
| C               | 15                   | 10                   | <5                   |
| D               | 70                   | 55                   | <5                   |
| ADAR2†‡         |                      |                      |                      |
| -1              | 15                   | 10                   | <10                  |
| +23             | 25                   | 15                   | <10                  |
| +24             | 45                   | 35                   | 10                   |

The editing sites have been described<sup>2–5,27</sup>. Values, given as mean ± s.d. (*n* = 3), indicate the percentage of the edited version for the different editing sites analysed in the three genotypes. Values were obtained from whole-brain RNA by differential oligonucleotide-mediated hybridization of cloned RT-PCR products to distinguish between an adenosine (unedited) and a guanosine (edited) at the individual editing sites.

\* Values from P14 mice with unmodified *GluR-B* alleles. All other values were from P40 mice with *GluR-B* alleles sequence modified at the Q/R site codon<sup>9</sup>.

† Values derived from the different peak heights for the two nucleotides in identical positions in DNA sequence chromatograms. Values from three mice were averaged and rounded to the nearest 5 or 0 position in each case.

‡ Sites +265 in hotspot2 and -2, +9 and +10 in ADAR2 were edited to <5% in wild type.

§ Flip and flop splice versions. As assessed from sequence chromatograms, the approximate representations of the flip forms were 50% for GluR-B, 75% for GluR-C and 65% for GluR-D; see ref. 27.

‡ Present address: Department of Biology, Massachusetts Institute of Technology, 77 Massachusetts Avenue, MA 02139, USA.

adenosine deaminase activity<sup>6</sup>. As determined from cloned polymerase chain reaction with reverse transcription (RT-PCR) products from brain RNA<sup>6</sup>, Q/R site editing in primary GluR-B transcripts was tenfold lower in *ADAR2*<sup>-/-</sup> than in wild-type mice (10% compared with 98%, Table 1). This identifies ADAR2 as the principal RNA-editing enzyme at the Q/R site. The remaining low level of Q/R site editing in GluR-B pre-mRNA cannot be mediated by the residual, enzymatically inactive, truncated ADAR2 protein, but is mediated by another ADAR, perhaps ADAR1 (refs 14, 18), for which gene expression appeared unchanged in *ADAR2*<sup>-/-</sup> mice (Fig. 1d).

The low extent of Q/R site editing of GluR-B pre-mRNA led to nuclear accumulation of incompletely processed primary GluR-B transcripts and to a fivefold reduction in GluR-B mRNA, as assessed by RNase protection (20 ± 5%; *n* = 3; Fig. 2a) and quantitative RT-PCR (20 ± 4% of wild type; *n* = 3; P14; not shown). The increased level of intron 11-containing GluR-B transcripts and the decrease in GluR-B mRNA were easily visualized by *in situ* hybridization (Fig. 2b). Editing is thus a prerequisite for efficient splicing and processing of the pre-mRNA. The edited GluR-B transcripts are preferentially spliced, as revealed by a shift in Q/R site editing from 10% to 40% when comparing intron-11-containing transcripts with GluR-B mRNA (Table 1). A defect in transcript processing caused by the interaction of the residual truncated ADAR2 protein with RNA can be excluded because GluR-B pre-mRNA accumulation is also

observed in *ADAR2*<sup>+/-</sup> mice expressing the Q/R site-uneditable *GluR-B*<sup>ΔECS</sup> allele<sup>11</sup>.

The fivefold drop in mRNA reduced GluR-B subunit levels similarly (21 ± 3% of wild type; *n* = 3; P14), as indicated by western analysis of brain protein from *ADAR2*<sup>-/-</sup> mice (Fig. 3a), and as visualized by immunocytochemistry in the hippocampal subfields (Fig. 3b). We also observed a moderate reduction in GluR-A protein (42 ± 5% of wild type; *n* = 3; Fig. 3a), barely detected by immunocytochemistry (Fig. 3b), with GluR-A mRNA being only slightly reduced (RNase protection: 83 ± 10% of wild type; *n* = 3; P14; Fig. 2a). The lower GluR-A protein levels may be a consequence of the severe reduction in GluR-B, the principal partner of GluR-A in AMPA receptor assembly<sup>9</sup>. Notably, mice lacking all GluR-A expression are phenotypically robust and normal in most respects<sup>19</sup>, precluding the possibility that the moderate GluR-A reduction contributes to the severe phenotype of *ADAR2*<sup>-/-</sup> mice. NMDA receptor<sup>10</sup> NR1 protein levels in *ADAR2*<sup>-/-</sup> mice appeared unchanged (data not shown).

As predicted from previous studies<sup>11,12,20</sup>, reduced expression and reduced Q/R site editing of GluR-B alters AMPA receptor channel properties mainly in principal neurones, which normally express fully edited GluR-B at levels sufficient for incorporation into most heteromeric AMPA receptors. Indeed, in accordance with the molecular analysis, AMPA receptor-mediated currents recorded in acute *ADAR2*<sup>-/-</sup> brain slices from nucleated patches of CA1

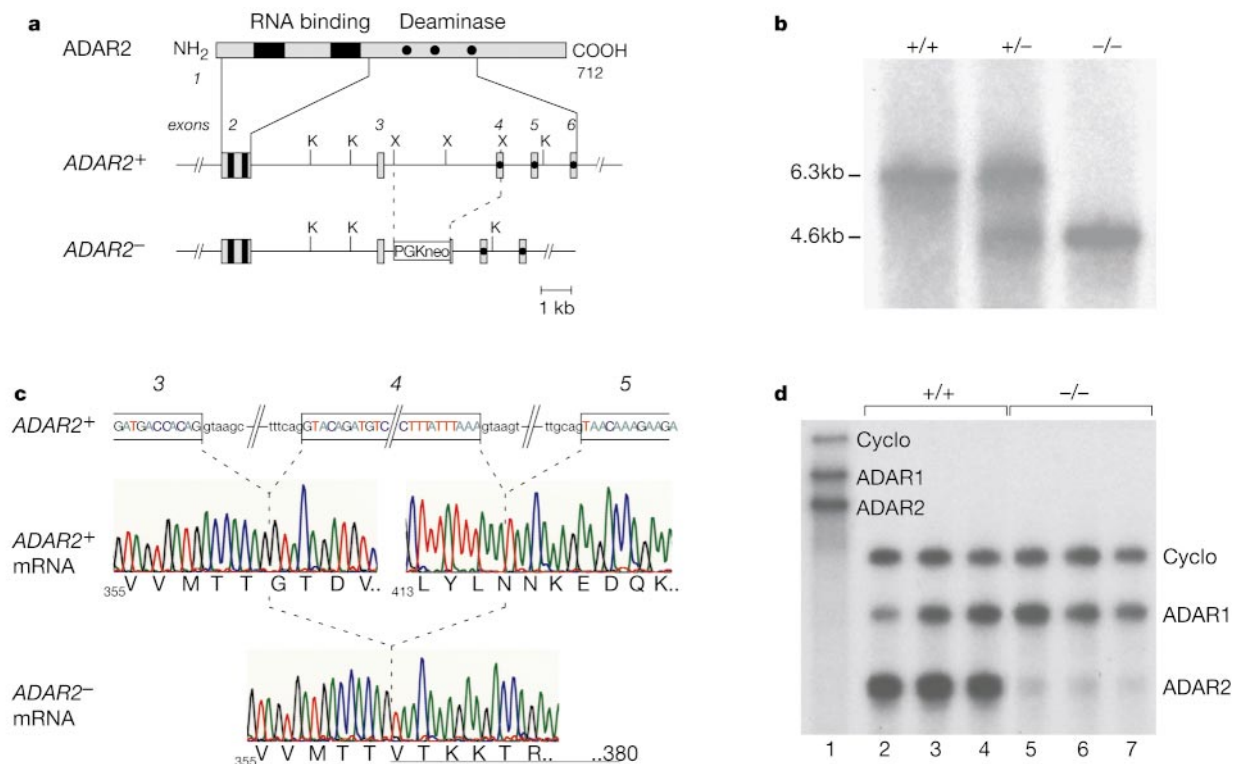


**Figure 1** Targeted *ADAR2* allele (Mouse Genome Database symbol, *Adarb1*) and transcript. **a**, Domain structure of the RNA-dependent adenosine deaminase ADAR2 and exon-intron organization of *ADAR2*<sup>+</sup> and *ADAR2*<sup>-</sup> alleles. Protein domains<sup>3,7</sup> are connected to their corresponding exons<sup>16</sup>. In the *ADAR2*<sup>-</sup> allele, most of intron 3 and exon 4 is replaced by *PGK-neo* (dashed lines). Filled boxes, double-stranded RNA-binding domains in protein and exons; filled circles, conserved sequences in deaminase domain of ADARs<sup>3</sup>. X, *XhoI*; K, *KpnI*. **b**, Southern analysis of *ADAR2* alleles in *KpnI*-restricted genomic DNA from mouse liver with a cDNA probe encoding residues 323–452 from exons 3–5. +/+, wild type; +/-, heterozygote; -/-, *ADAR2*-deficient homozygote. **c**, DNA sequence analysis of RT-PCR products from *ADAR2*<sup>+</sup> and *ADAR2*<sup>-</sup> mRNAs. A segment with exons 3–5 of the *ADAR2*<sup>+</sup> allele depicts nucleotides coloured as in chromatograms for wild-type

and mutant cDNA sequences. Amino acids are given as single letters, numbered according to ADAR2. Exon sequence deleted in *ADAR2*<sup>-</sup> is indicated by stippled lines. Note the frameshift caused by exon 4 deletion (underlined grey residues). **d**, RNase protection with whole-brain RNA by mRNAs for cyclophilin (Cyclo) as internal standard, ADAR1, and ADAR2 in three wild-type (+/+) and three *ADAR2*-deficient (-/-) mice. Lane 1, unprotected radiolabelled antisense RNA probes for cyclophilin (324 nt), ADAR1 (283 nt) and ADAR2 (248 nt). Lanes 2–7, protected probe fragments for cyclophilin (244 nt), ADAR1 (203 nt, exon 6–7 sequences<sup>25</sup> encoding RNA-binding domains) and ADAR2 (168 nt, exons 2–3 sequences<sup>16</sup> for RNA-binding domains). A probe derived from ADAR2 exon 6–7 sequences<sup>16</sup> for part of the deaminase domain yielded the same reduction for *ADAR2*<sup>-</sup> allele expression (not shown).

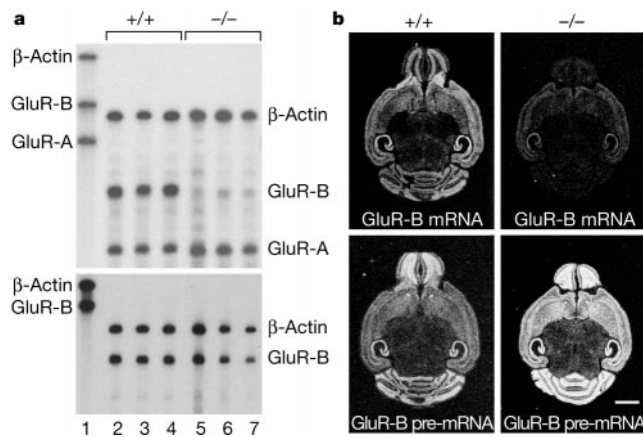


**Figure 2** GluR-B and GluR-A transcript analyses. **a**, RNase protection. Lane 1, unprotected radiolabelled antisense RNA probes for  $\beta$ -actin as internal standard (334 nt), GluR-B<sup>26</sup> (upper gel, 270 nt; lower gel, 272 nt) and GluR-A (221 nt); lanes 2–4, protection by whole-brain RNA from P14 *ADAR2*<sup>+/+</sup> mice (+/+); lanes 5–7, from P14 *ADAR2*<sup>-/-</sup> mice (-/-). Protected fragment sizes in nt:  $\beta$ -actin, 245; GluR-B, 190 (upper gel, exons 11–12) and 192 (lower gel, exons 3–4); GluR-A, 141 (exons 3–4). Note the reduction in

GluR-B mRNA in the mutant is only revealed with the exon 11–12 probe (upper gel), but not with the exon 3–4 probe (sum of pre- and mRNA; lower gel). **b**, *In situ* hybridization. Horizontal brain sections of *ADAR2*<sup>+/+</sup> and *ADAR2*<sup>-/-</sup> mice were hybridized with <sup>35</sup>S-labelled oligonucleotide probes<sup>24</sup> specific for GluR-B mRNA (36 nt, spanning exons 11–12) and pre-mRNA (37 nt, intron 11). Note the substantially higher levels of GluR-B pre-mRNA in the mutant and of GluR-B mRNA in wild type. Scale bar, 2 mm.

pyramidal cells and other principal neurones (cerebellar Purkinje cells and neocortical layer 5 pyramidal neurones) displayed, relative to wild type, pronounced rectification, increased desensitization rates and 30-fold higher Ca<sup>2+</sup> permeability ( $P_{Ca}/P_{Na}$  3.34–3.94 ( $n = 4–8$ ) compared with 0.12–0.14 ( $n = 4–10$ )). Moreover, the macroscopic AMPA receptor-mediated conductance in CA1 pyramidal cells of *ADAR2*<sup>-/-</sup> mice was significantly higher ( $40.8 \pm 4.0$  ( $n = 10$ ) compared with  $21.4 \pm 3.0 \mu S$  ( $n = 3$ ) in wild type) than in our mouse mutants expressing editing-deficient *GluR-B* genes<sup>11,12</sup>. As reported<sup>12</sup>, the increase in macroscopic AMPA conductance, caused by the higher single-channel conductance in absence of GluR-B(R) participation<sup>10</sup>, appears to be the primary cause for the high seizure susceptibility of young mice expressing Q/R site-unedited GluR-B transcripts.

To show that the prematurely lethal phenotype of *ADAR2*<sup>-/-</sup> mice

is engendered by insufficient Q/R site editing of GluR-B, we attempted a rescue of this phenotype by introducing a *GluR-B*<sup>R</sup> allele<sup>9</sup>. This allele, generated by targeting, contains an arginine (R) codon for the Q/R site, and its expression in *ADAR2*<sup>-/-</sup> mice is independent of Q/R site editing. We found that the severely compromised phenotype of *ADAR2*<sup>-/-</sup> mice was partially rescued already in heterozygous *ADAR2*<sup>-/-</sup>/*GluR-B*<sup>R/R</sup> mutants, which survived up to P35 (Fig. 4). Moreover, their phenotype was less impaired than that of *GluR-B*<sup>+/ $\Delta$ ECS</sup> mice, consistent with the hypothesis that phenotypic impairment increases with the Q/R ratio of GluR-B<sup>12</sup>. In both *ADAR2*<sup>-/-</sup>/*GluR-B*<sup>R/R</sup> and *GluR-B*<sup>+/ $\Delta$ ECS</sup> mutants, one GluR-B allele expresses exclusively GluR-B(R), but primary transcripts from the second allele are underedited and the corresponding mRNA levels are reduced. In mRNA derived from the *GluR-B* <sup>$\Delta$ ECS</sup> allele the Q/R site is not edited at all, whereas mRNA from the *GluR-B*<sup>+</sup> allele is Q/R site edited to 40% in the *ADAR2*<sup>-/-</sup> background. Thus, the Q/R ratio in GluR-B-containing AMPA receptors is lower in *ADAR2*<sup>-/-</sup>/*GluR-B*<sup>R/R</sup> than in *GluR-B*<sup>+/ $\Delta$ ECS</sup>

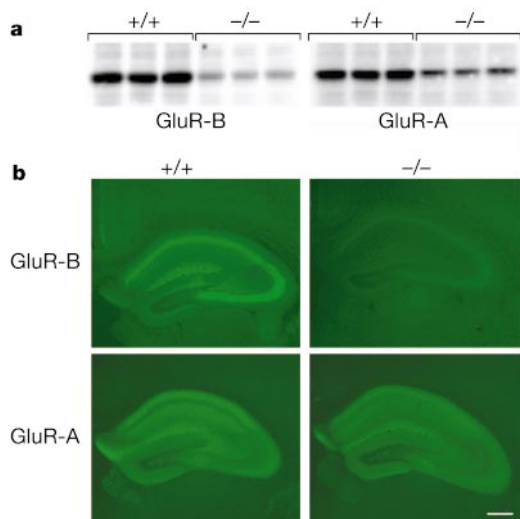


**Figure 3** GluR-B and GluR-A protein analyses. **a**, Western blots of brain protein from three *ADAR2*<sup>+/+</sup> (+/+) and three *ADAR2*<sup>-/-</sup> (-/-) mice with antibodies for two AMPA receptor subunits. **b**, Immunocytochemistry showing blow-ups of the hippocampus in coronal vibratome sections (40  $\mu m$ ) of P14 *ADAR2*<sup>+/+</sup> and *ADAR2*<sup>-/-</sup> brains, probed with antibodies to GluR-B (upper panels) and GluR-A (lower panels) and stained with FITC-conjugated secondary antibody. Note that a moderate GluR-A reduction is apparent in **a**, but barely detectable in **b**. Scale bar, 0.3 mm.

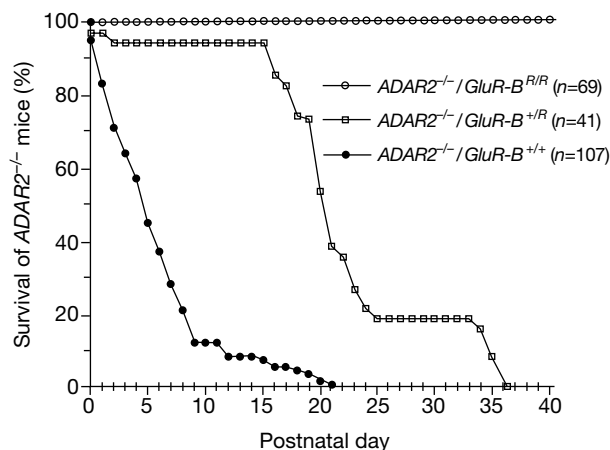


**Figure 4** Survival of *ADAR2*<sup>-/-</sup> mice. Data points depict the percentage of mice alive at the indicated postnatal days. The number of mice observed is listed in parentheses for each genotype. Note that the life span of *ADAR2*-deficient mice increased with the copy number of the sequence-modified *GluR-B*<sup>R</sup> allele, entirely consistent with the reduction in Q/R ratio, as elucidated by previous studies on the effect of Q/R site-uneditable *GluR-B* alleles in targeted mouse mutants<sup>11,12</sup>.

mice, and the phenotype is less affected. Full rescue of the impaired *ADAR2*<sup>-/-</sup> phenotype was achieved after introducing the second *GluR-B*<sup>R</sup> allele. *ADAR2*<sup>-/-</sup>/*GluR-B*<sup>R/R</sup> mice appeared normal at all ages, like *GluR-B*<sup>R/R</sup> mice<sup>9</sup>, as judged by food intake, weight increase, postnatal development, breeding and general behaviour. This identifies the *GluR-B* transcript as the most critical substrate for *ADAR2* in the mammal.

We investigated whether RNA editing at other known sites is affected by functional *ADAR2* ablation. We observed reduced editing at the majority of 25 positions in diverse transcripts (Table 1); even hemizygoty for *ADAR2* led at several sites to a modest decline in the extent of editing (Table 1). Notably, the actual reduction in the extent of editing may not have been revealed, as many of the sites were analysed at the mRNA rather than the pre-mRNA stage. Nevertheless, the results indicate a pleiotropic action of *ADAR2*, not entirely anticipated from *in vitro* studies<sup>14,21</sup>; *ADAR2* may act in concert with other RNA-editing enzymes, perhaps assembled with additional RNA interacting proteins in a multi-component nuclear 'editosome'. The reduced editing at many sites might also reflect, at least in part, interference with other *ADARs* by the residual truncated *ADAR2* protein (Fig. 1c); if so, affected editing levels might not indicate true catalysis by *ADAR2*. The severe reduction in transcript levels from the mutant allele (Fig. 1d), however, may render such interference unlikely.

In summary, we have shown that RNA editing can control the rate of splicing in nuclear transcripts; a link between editing and splicing has also been reported in *Drosophila*<sup>22</sup>. Moreover, our study identified the Q/R site codon in *GluR-B* pre-mRNA as a critical physiological substrate of *ADAR2*, apparently the only one at which editing is essential for viability, at least during the first few weeks of life. Whether or not dependence of viability on Q/R site editing extends into adulthood will be investigated by conditional *ADAR2* gene expression. As *ADAR2*<sup>-/-</sup> mice were phenotypically rescued by *GluR-B*<sup>R</sup> alleles, the effects caused by underediting of other *ADAR2* substrates need to be elucidated by future analyses of *ADAR2*<sup>-/-</sup>/*GluR-B*<sup>R/R</sup> mice. □

## Methods

### Extent of editing

RT-PCR products from brain RNA of the different genotypes were generated with primers specific for the pre-mRNAs or mRNAs (details of oligonucleotides are available from the author on request). Amplicons were cloned directionally into M13 RF DNA and more than 1,000 recombinant single-stranded phage plaques were hybridized to oligonucleotide probes that distinguish between edited and unedited positions in the different sequences<sup>6</sup>. Alternatively, amplicons were sequenced directly, and the approximate extent of editing was derived from the different peak heights for the two nucleotides occurring in identical positions in DNA sequence chromatograms.

### *GluR-B* mRNA levels by RT-PCR

RT-PCR was used with primers to co-amplify all four AMPA receptor subunit cDNAs<sup>23</sup>. Amplicons were cloned directionally, and filters containing more than 1,000 recombinant phage plaques were probed sequentially for the different subunit cDNAs. The numeric representations (in percent) of the four subunit sequences were for *ADAR2*<sup>-/-</sup> mice: *GluR-A*, 57; *GluR-B*, 14; *GluR-C*, 20; *GluR-D*, 9; for *ADAR2*<sup>+/-</sup> mice 36, 41, 15, 8, and for wild-type mice 39, 44, 11, 6.

### RNase protection

RNase protection (RPALIII Ribonuclease protection assay kit, Ambion) was used to determine transcripts levels for *GluR-A*, *GluR-B*, *ADAR1* and *ADAR2*. Individual reactions were performed with 20 µg total whole-brain RNA, and radiolabelled antisense RNA probes were as described in Fig. 2.

### *In situ* hybridization

*In situ* hybridization was performed on horizontal cryostat sections of P14 mouse brains with 3'-end-labelled oligonucleotides<sup>24</sup>. Exposure to X-ray film was for 7 days. Control sections hybridized with labelled probe in presence of a 100-fold excess of the unlabelled oligonucleotide generated no signal.

### Western analysis and immunocytochemistry

Western blots with 10 µg of P14 whole-brain protein extracts per lane were successively

probed, after intermittent stripping, with antibodies to *GluR-B* (1:200; Pharmingen) and *GluR-A* (1:300; Chemicon); secondary antibody was conjugated to horseradish peroxidase (1:40,000; Amersham) and detection was with Super Signal West (Pierce). P14 brain sections were processed for immunocytochemistry<sup>19</sup>, incubated with antibodies to *GluR-B* (1:10) and *GluR-A* (1:50) and stained with FITC-conjugated goat anti-rabbit IgG (1:100; Jackson ImmunoResearch).

## Electrophysiology

AMPA receptor-mediated currents in whole-soma 'nucleated' patches of identified neurones in acute brain slices of P14 mice were elicited and analysed as described<sup>12</sup>.

Received 10 March; accepted 22 May 2000.

- Bass, B. L. RNA editing. An I for editing. *Curr. Biol.* **5**, 598–600 (1995).
- Rueter, S. & Emeson, R. in *Modification and Editing of RNA* (eds Grosjean, H. & Benne, R.) 343–361 (ASM, Washington DC, 1998).
- Seeburg, P. H., Higuchi, M. & Sprengel, R. RNA editing of brain glutamate receptor channels: mechanism and physiology. *Brain Res. Rev.* **26**, 217–229 (1998).
- Burns, C. M. *et al.* Regulation of serotonin-2C receptor G-protein coupling by RNA editing. *Nature* **387**, 303–308 (1997).
- Rueter, S. M., Dawson, T. R. & Emeson, R. B. Regulation of alternative splicing by RNA editing. *Nature* **399**, 75–79 (1999).
- Higuchi, M. *et al.* RNA editing of AMPA receptor subunit *GluR-B*: A base-paired intron–exon structure determines position and efficiency. *Cell* **75**, 1361–1370 (1993).
- Melcher, T. *et al.* A mammalian RNA editing enzyme. *Nature* **379**, 460–464 (1996).
- Bass, B. L. *et al.* A standardized nomenclature for adenosine deaminases that act on RNA. *RNA* **3**, 947–949 (1997).
- Kask, K. *et al.* The AMPA receptor subunit *GluR-B* in its Q/R site-unedited form is not essential for brain development and function. *Proc. Natl Acad. Sci. USA* **95**, 13777–13782 (1998).
- Dingledine, R., Borges, K., Bowie, D. & Traynelis, S. F. The glutamate receptor ion channels. *Pharmacol. Rev.* **51**, 7–61 (1999).
- Brusa, R. *et al.* Early-onset epilepsy and postnatal lethality associated with an editing-deficient *GluR-B* allele in mice. *Science* **270**, 1677–1680 (1995).
- Feldmeyer, D. *et al.* Neurological dysfunctions in mice expressing different levels of the Q/R site-unedited AMPAR subunit *GluR-B*. *Nature Neurosci.* **2**, 57–64 (1999).
- Melcher, T. *et al.* RED2, a brain-specific member of the RNA-specific adenosine deaminase family. *J. Biol. Chem.* **271**, 31795–31798 (1996).
- Maas, S. *et al.* Different structural and enzymatic requirements for RNA editing in glutamate receptor pre-mRNAs. *J. Biol. Chem.* **271**, 12221–12226 (1996).
- Lai, F., Chen, C. X., Carter, K. C. & Nishikura, K. Editing of glutamate receptor B subunit ion channel RNAs by four alternatively spliced DRADA2 double-stranded RNA adenosine deaminases. *Mol. Cell. Biol.* **17**, 2413–2424 (1997).
- Villard, L., Tassone, F., Haymowicz, M., Welborn, R. & Gardiner, K. Map location, genomic organization and expression patterns of the human RED1 RNA editase. *Somat. Cell. Mol. Gen.* **23**, 135–145 (1997).
- Nagy, A., Rossant, J., Nagy, R., Abramow-Newerly, W. & Roder, J. C. Derivation of completely cell culture-derived mice from early-passage embryonic stem cells. *Proc. Natl Acad. Sci. USA* **90**, 8424–8428 (1993).
- Dabiri, G. A., Lai, F., Drakas, R. A. & Nishikura, K. Editing of *GluR-B* ion channel RNA in vitro by recombinant double-stranded RNA adenosine deaminase. *EMBO J.* **15**, 34–45 (1996).
- Zamantillo, D. *et al.* Importance of AMPA receptors for hippocampal synaptic plasticity but not for spatial learning. *Science* **284**, 1805–1811 (1999).
- Jia, Z. *et al.* Enhanced LTP in mice deficient in the AMPA receptor *GluR2*. *Neuron* **17**, 945–956 (1996).
- Herb, A., Higuchi, M., Sprengel, R. & Seeburg, P. H. Q/R site editing in kainate receptor *GluR5* and *GluR6* pre-mRNAs requires distant intronic sequences. *Proc. Natl Acad. Sci. USA* **93**, 1875–880 (1996).
- Reenan, R. A., Hanrahan, C. J. & Ganetzky, B. The *mLenaps* RNA helicase mutation in *Drosophila* results in a splicing catastrophe of the *para* Na<sup>+</sup> channel transcript in a region of RNA editing. *Neuron* **25**, 139–149 (2000).
- Geiger, J. R. P. *et al.* Relative abundance of subunit mRNAs determines gating and Ca<sup>2+</sup> permeability of AMPA receptors in principal neurons and interneurons in rat CNS. *Neuron* **15**, 193–204 (1995).
- Wisden, W. & Morris, B. J. in *In Situ Protocols for the Brain* (eds Wisden, W. & Morris, B. J.) 9–30 (Academic, London, 1994).
- Wang, Y., Zeng, Y., Murray, J. M. & Nishikura, K. Genomic organization and chromosomal localization of the human dsRNA adenosine deaminase gene: the enzyme for glutamate-activated ion channel RNA editing. *J. Mol. Biol.* **254**, 184–195 (1995).
- Köhler, M., Kornau, H. -C. & Seeburg, P. H. The gene for the principal AMPA receptor subunit *GluR-B*: organization and sequences for alternatively spliced and edited transcripts. *J. Biol. Chem.* **269**, 17367–17370 (1994).
- Lomeli, H. *et al.* Control of kinetic properties of AMPA receptor channels by nuclear RNA editing. *Science* **266**, 1709–1713 (1994).

## Acknowledgements

We thank R. Wenthold for the antibody to *GluR-B*; A. Nagy for the murine embryonic stem cell line R1; K. Kask for help with *GluR-B*<sup>R</sup> mice; F. Zimmermann for blastocyst injection; S. Grünwald and H. Grosskurth for DNA sequencing; U. Amtmann for *in situ* hybridization; and H. Avci, C. Faul and C. Baust for technical help. This work was supported, in part, by the Deutsche Forschungsgemeinschaft, the Human Frontier Science Program and the Bristol-Myers Squibb foundation.

Correspondence and requests for materials should be addressed to P.H.S. (e-mail: seeburg@mpimf-heidelberg.mpg.de).